Available online at www.sciencedirect.com
ScienceDirect
Journal of Power Sources 161 (2006) 1225–1233
JOURNAL OF POWER SOURCES
www.elsevier.com/locate/jpowsour

# Characteristics of hydrogen produced by partial oxidation and auto-thermal reforming in a small methanol reformer

Rong-Fang Horng [a,*], Huann-Ming Chou [a], Chiou-Hwang Lee [b], Hsien-Te Tsai [a]

[a] *Department of Mechanical Engineering, Clean Energy Center, Kun Shan University, No. 949 Da-Wan Rd., Yung-Kang City, Tainan County 710, Taiwan*
[b] *Material and Chemical Laboratories, Industrial Technology Research Institute, Hsinchu, Taiwan*

Received 27 April 2006; received in revised form 22 May 2006; accepted 6 June 2006
Available online 28 July 2006

**Abstract**

This paper investigates experimentally, the transient characteristics of a small methanol reformer using partial oxidation (POX) and auto-thermal reforming (ATR) for fuel cell applications. The parameters varied were heating temperature, methanol supply rate, steady mode shifting temperature, $O_2$/C ($O_2$/$CH_3OH$) and S/C ($H_2O$/$CH_3OH$) molar ratios with the main aim of promoting a rapid response and a high flow rate of hydrogen.

The experiments showed that a high steady mode shifting temperature resulted in a faster temperature rise at the catalyst outlet and vice versa and that a low steady mode shifting temperature resulted in a lower final hydrogen concentration. However, when the mode shifting temperature was too high, the hydrogen production response was not necessarily improved. It was subsequently shown that the optimum steady mode shifting temperature for this experimental set-up was approximately 75 °C. Further, the hydrogen concentration produced by the auto-thermal process was as high as 49.12% and the volume flow rate up to 23.0 L min$^{-1}$ compared to 40.0% and 20.5 L min$^{-1}$ produced by partial oxidation.


*Keywords:* Methanol reformer; Partial oxidation reforming; Auto-thermal reforming; Steady mode shifting temperature

## 1. Introduction

Hydrogen can be produced from the reformation of hydrocarbons such as methanol, natural gas or oil [1] by means of partial oxidation (POX), auto-thermal (ATR) and steam reforming etc. Because of its characteristic ease in reforming and its low reaction temperature, methanol is the most suitable fuel for reforming [2].

In Taiwan, Sung [3] performed theoretical and experimental studies on methanol reformers and concluded that the methanol conversion efficiency increased with the temperature of the reformer as did the CO concentration. The optimum outlet temperature of the reformer was proposed to be between 180 and 310 °C. With a methane steam reformer, Sung [4] revealed that the CO concentration was within the requirement level for a fuel cell and proposed a moderate value for the S/C ratio for conserving energy for vaporizing water. He proposed that future work focus on investigating cold start and varying load conditions. Using a small methanol reformer with a metallic catalyst covered by Cu–ZnO/$Al_2O_3$, Chen [5] carried out an extensive parametric study and concluded that the optimum operating condition was with an S/C (water–methanol) molar ratio of 1.8 and an $O_2$/C (molecular oxygen to methanol) molar ratio of 0.2.

Höhlein et al. [6] designed and operated a methanol steam reformer at different temperatures. They focused on a methanol reformer for on-board hydrogen generation. They found intricate relationships between the CO emission level, the heating mode and variations of the reformer temperature. However, the start-up characteristics of the reformer did not satisfy expectations. The methanol steam reformer developed by Emonts et al. [7] was aimed at a low specific weight, a quick start-up, low emission and high efficiency. The specific weight of 4 kg kW$^{-1}$ and a 50% electricity generation efficiency were achieved. It was also revealed that the CO emissions increased with operating temperature. Wiese et al. [8] investigated the steady, dynamic and start-up conditions of a methanol steam reformer that commenced reaction only after 8 min from cold start. For a 3 kW methanol reformer that achieved a thermal efficiency as high as 89%, Han et al. [2] concluded that the maximum hydrogen production occurred after 15 min from cold

* Corresponding author. Tel.: +886 6 205 0496; fax: +886 6 205 0509.
*E-mail address:* hong.rf@msa.hinet.net (R.-F. Horng).

0378-7753/$ – see front matter © 2006 Elsevier B.V. All rights reserved.
doi:10.1016/j.jpowsour.2006.06.043

start. Nagano et al. [9] studied catalytic methanol steam reforming by simulation and experiment and demonstrated a trade-off relationship between methanol conversion and CO concentration. The trade-off relationship was improved by enhancing heat transfer through an internal corrugated metal heater and an external catalytic combustion heater. Takeda et al. [10] successfully enhanced the reaction speed of the catalyst by coupling electric heating and steam reforming in a methanol reformer and combining heating by heaters with the aim of improving vaporisation of the liquid fuel and water. Choi and Stenger [11] employed a Cu–ZnO/$Al_2O_3$ catalyst to investigate the effect of water addition on the hydrogen production characteristics with methanol as fuel. Despite achieving 100% methanol conversion efficiency without water, they demonstrated that by adding water, a higher hydrogen concentration and a lower CO concentration could be achieved. Holladay et al. [12] manufactured a small size methanol reformer for steam reforming and attained 99% conversion efficiency at 360 °C with an S/C ratio of 1.8. Lindström et al. [13] developed an onboard vehicle methanol reformer that activated the catalyst within 4–6 min under the combined operations of partial oxidation and steam reforming. Löffler et al. [14] developed a set of reformers, one of which was a pre-reformer that promoted the time to achieve the reaction temperature of the catalyst through heat from partial oxidation. The main reformer then underwent steam reforming and was shown to produce high thermal efficiency and high hydrogen purity. Horng [15] designed and manufactured a small methanol reformer for studying its cold start characteristics. The time taken for the reformer to produce hydrogen from cold start was 220 s, with hydrogen production reaching stability within 4–5 min. Springmann et al. [16] built a simulation model of cold start for a gasoline fuel processor. They concluded that the air-fuel mixture control and heat-up by oxidation could reduce cold start time significantly, and a cold start of the reforming unit below one minute was possible. Goebel et al. [17] studied a fast starting gasoline fuel processor. They found that a start-up time of 140 s to full power as fueled with hydrogen for catalyst light-off, and a start method of fuel lean in gasoline was achieved with full power within 190 s. Ahmed et al. [18] studied the fast-start strategy on a gasoline fuel processor by experiment and simulation. They thought that using a small amount of electrical energy, igniting the fuel-air mixture on the reformer in the partial oxidation mode, then switching to the auto-thermal mode was a promising way to start the reformer quickly.

It is clear from Ref [15] that more effort is still needed to improve the cold-start and transient characteristics of the reformer as an onboard vehicle fuel processor. As a continuation of this work, the objective of this study is to design a 3 kW methanol reformer that is quick in response to reach a catalyst light-off temperature and thus render it highly suitable for use in fuel cells. The same method of shifting from partial oxidation reforming to auto-thermal reforming once the reformer reached the light-off status is employed to increase hydrogen production. Therefore, the transient response of transition from partial oxidation to auto-thermal reforming is also investigated in this study.

Table 1
Specifications of the reformer

| | |
|---|---|
| Main body | |
| Reaction chamber | 124Ø mm stainless steel |
| Height | 510 mm |
| Nozzle | Fuel and air |
| Heater | 120 W × 8 glow plugs |
| Power supply for heater | 12VDC |
| Catalyst | |
| Substrate | Ceramic |
| Diameter | 117Ø mm |
| Length | 50 mm |
| Composition | Pt and Cu–ZnO/$Al_2O_3$ |
| Cell number | 400 cells $in^{-2}$ |
| Surface/volume ratio | 2547 $m^{-1}$ |

## 2. Experimental method and procedure

### 2.1. Experimental set-up

A purpose-designed methanol reformer composed of a fuel supply system, a temperature controlling system and a gas sampling system was constructed. The catalyst of the reformer, whose specifications are listed in Table 1, was provided by the Heterogeneous Catalysis Department in the Material and Chemical Laboratories of the Industrial Technology Research Institute of Taiwan. The catalyst covered the honeycombed ceramic substrate as a wash-coated layer whose main composition was Pt and the mixed oxide, Cu–ZnO/$Al_2O_3$. The fuel supply system consisted mainly of a methanol and an air supply system. The former was made up of an electrical fuel pump, pressure regulators, flowmeter and fuel nozzle whilst the latter consisted of a single and a multi-hole nozzle in addition to a pressure regulator, a flowmeter and an air compressor with filters. The flow temperature control system included glow plugs, a temper-

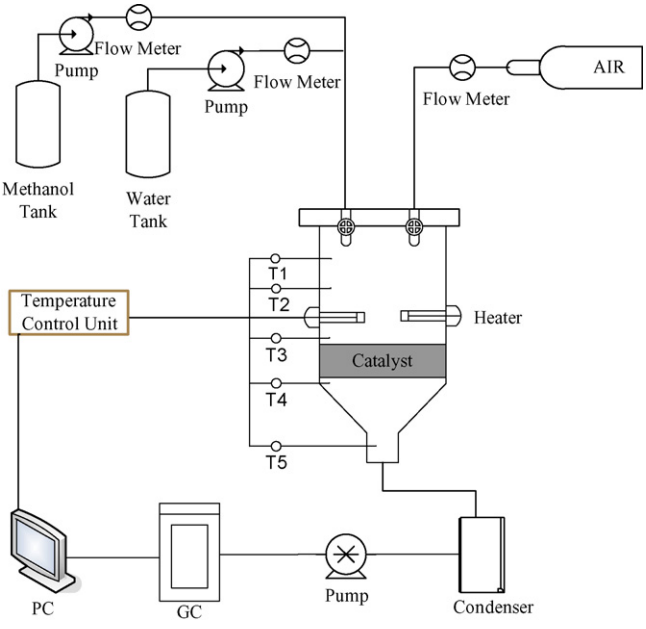


Fig. 1. Schematic of the methanol reformer set-up.

ature controller and a temperature-recording device. The input air temperature of the catalyst was regulated by eight 120 W glow plugs, contributing a total of 960 W. A heating power of 240 W was applied for partial oxidation reforming at the start of ignition. However, once water is added, the process is shifted to auto-thermal reforming, the heating power was increased to between 400 and 960 W for an S/C ratio of 0.68–1.29 for compensating for the latent heat of evaporation of water. The K-type thermocouples were installed before and after the fuel spray, at the inlet and the outlet of the catalyst. The temperature at the outlet of the catalyst ($T_4$) was used as the feedback for the temperature control system. The gas analyzing system included an Agilent 6850 GC, condenser, a sampling pump, sampling bags and a micro syringe. The schematic of the experimental set-up is shown in Fig. 1.

### 2.2. Experimental method and relative calculations

The operating parameters that promoted the reaction response of the methanol reformer from cold start were determined through partial oxidation. The parameters included heating power, heating temperature, $O_2$/C molar ratio, methanol supply rate, air flow rate and steady mode shifting temperature. The air supply rate was varied with the methanol supply rate, and air must be injected into the reformer before the methanol. Further, the main variable in the transient to steady mode shifting process was the air flow rate. When the temperature of the catalyst outlet reached the specified value of 30, 50, 75, 100, 150, 200 or 250 °C, the air supply rate was changed from the original supply rate at cold start to a steady supply rate for producing the maximum hydrogen concentration. This temperature is defined as the steady mode shifting temperature. The gas chromatograph was fully warmed up prior to each test. As soon as the data recorder was activated, the heating system for pre-heating air that was to be injected into the chamber was switched on. After 10 s, methanol was injected through the nozzle and a gas sample of the emission was taken every 60 s for analysis until the gas production stabilized. The air supply procedure from cold start is illustrated in Fig. 2. When the catalyst outlet temperature reached the pre-set heating temperature, the air supply rate was reduced to the steady mode. This was to set the $O_2$/C ratio for steady operation. To ensure that the main body of the reformer cooled to room temperature before the next test, the minimum time between tests was 6 h.

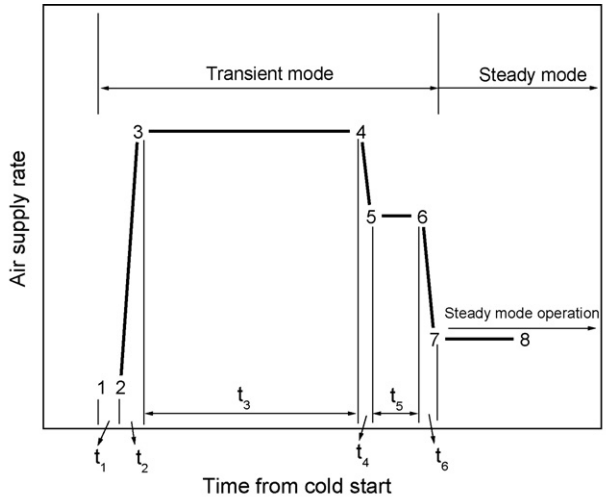


Operating duration and air supply rates from cold start for different methanol supply rates

| Time interval | Methanol supply rate cc min$^{-1}$--(mol min$^{-1}$) | | | | | |
|---|---|---|---|---|---|---|
| | 15.8--(0.40) | | 25.5--(0.64) | | 30.3--(0.76) | |
| | time sec | Air flow rate mol min$^{-1}$ | time sec | Air flow rate mol min$^{-1}$ | time sec | Air flow rate mol min$^{-1}$ |
| $t_1$ | 10 | 0.4 | 10 | 0.4 | 10 | 0.4 |
| $t_2$ | 1.0-1.5 | | 1.0-1.5 | | 1.0-2.0 | |
| $t_3$ | * | 2.41 | * | 2.81 | * | 3.22 |
| $t_4$ | 1.0-1.5 | | 1.0-1.5 | | 1.0-1.5 | |
| $t_5$ | ** | *** | ** | *** | ** | *** |
| $t_6$ | 1.0-1.5 | 0.70 | 1.0-1.5 | 0.85 | 1.0-1.5 | 0.94 |

* Set from when the catalyst outlet temperature reached the pre-set heating temperature.
** Changed to steady mode after the catalyst outlet temperature reached the target temperature.
*** Air flow decreased until the explosion ceased

Fig. 2. Air supply procedure for the methanol reformer from cold start.

The gas chromatograph was calibrated by feeding in and analyzing three different known concentrations of a standard gas that yielded a coefficient of linear regression, $R^2$, of above 0.999. Based on this calibration curve, the composition of the emission from the reformer could be determined. A SUPELCO 1-2390-U column was used. The gas chromatograph was set to have a companion fluid flow rate of 10 cc min$^{-1}$, an inlet temperature of 100 °C, an oven temperature of 160 °C and a detector temperature of 200 °C.

Relative calculations

(1) Partial oxidation reforming

Theoretical reaction

$$CH_3OH_{(g)} + \tfrac{1}{2}(O_{2(g)} + 3.76N_{2(g)}) \rightarrow CO_{2(g)} + 2H_{2(g)} + 1.88N_{2(g)},$$
$$\Delta H = -192.2\,\text{kj/mol} \quad (1.1)$$

Real reaction

$$x_1CH_3OH_{(l)} + z_1(O_{2(g)} + 3.76N_{2(g)}) \rightarrow a_1CO_{2(g)} + b_1CO_{(g)} + c_1H_{2(g)} + d_1O_{2(g)} + e_1CH_{4(g)} + f_1N_{2(g)} + g_1H_2O_{(g)}, \quad \Delta H \quad (1.2)$$

(2) Auto-thermal reforming

Theoretical reaction

$$CH_3OH_{(g)} + (1-x)H_2O_{(g)} + \tfrac{1}{2} \times (O_{2(g)} + 3.76N_{2(g)}) \rightarrow CO_{2(g)} + (3-x)H_{2(g)} + 1.88N_{2(g)}, \quad \Delta H \quad (2.1)$$

Real reaction

$$x_2CH_3OH_{(l)} + yH_2O_{(l)} + z_2(O_{2(g)} + 3.76N_{2(g)}) \rightarrow a_2CO_{2(g)} + b_2CO_{(g)} + c_2H_{2(g)} + d_2O_{2(g)} + e_2CH_{4(g)} + f_2N_{2(g)} + g_2H_2O_{(g)}, \quad \Delta H \quad (2.2)$$

As partial oxidation reforming is an exothermic reaction, apart from the ignition power, no accessory heating power is needed. Auto-thermal reaction has reactants consisting of methanol, air and water, and requires an accessory heating power for compensating the latent heat of water. $\Delta H$ (enthalpy of reaction) in Eqs. (1.2), (2.1) and (2.2) depend on the moles of water added or the moles of the gases produced. The equilibrium coefficients of $a_i$–$f_i$ in Eqs. (1.2) and (2.2) were measured by dry base analysis.

## 3. Results and discussion

Horng et al. [19] demonstrated that increasing the heating power increased the temperature at the heating section due to major combustion of the methanol-air mixture promoted by more hot spots of the glow plugs. This, however, also resulted in simultaneous rapid heat loss and therefore less heat transferred to the catalyst as shown by the moderate increase in the catalyst temperature for a given methanol supply rate. Lowering the heating power, on the other hand, resulted in a slower combustion rate of the gas mixture but the heat lost in the heating section was not as rapid due to the 'after burning' phenomenon. That is, the oxidation of the retained methanol continued to release heat to rapidly raise the temperature at the catalyst to the light-off temperature. For this reason, the lower heating power of 240 W was selected in this series of tests.

### 3.1. Partial oxidation reforming

Fig. 3 shows the relationship between the power supplied by heaters and methanol oxidation and the catalyst outlet temperature under different methanol supply rates for a heating power 240 W. In the figure, the heating temperature, i.e. the catalyst outlet temperature, was set at 100 °C, an indicator for when the heaters were to be switched off. After which, heating of the catalyst was solely provided by oxidation of the methanol oxidation. Further, the steady mode shifting temperature was set as 250 °C, therefore, the $O_2$/C ratio of air–methanol mixture was set as higher than that for normal reforming for hydrogen production. In this figure, the heat release rate from methanol oxidation is distinct. A higher heat release rate is obtained with a higher methanol supply rate. It is also clear that the heat release rate and temperature curves are similar for a methanol supply rate of between 25.5 and 30.3 cc min$^{-1}$. Notably, however, a slow temperature rise is observed for a methanol supply rate of 15.8 cc min$^{-1}$ due to a low heat release rate. When the operation is shifted to the steady mode, i.e., the air supply rate is decreased and the $O_2$/C ratio is reduced to the value for hydrogen production, the heat release rate from the methanol oxidation rapidly reduces to under 1 kW. At the same time, the catalyst outlet temperature also increases rapidly solely from the oxidation heat and reaches the light-off status without electric heating.

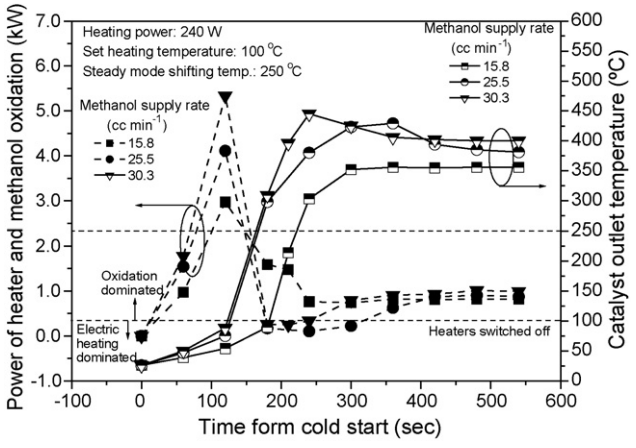


Fig. 3. Powers supplied by heaters and methanol oxidation and catalyst outlet temperature under different methanol supply rate for a heating power of 240 W.

Fig. 4 compares the shortest time taken for the catalyst outlet to reach 200 °C from cold start under varying methanol supply rates. It is evident from the figure that the time taken decreases with increasing methanol supply rate. The optimal cold start effect is attained under the combination of a methanol supply rate of 30.3 cc min$^{-1}$, 240 W heating power and an air supply rate of 80 L min$^{-1}$. A similar but less efficient result is obtained for the setting of 25.5 cc min$^{-1}$ methanol supply rate, a heating power of 240 W and an air supply rate of 70 L min$^{-1}$. It is noted that for the latter setting, when the methanol supply rate is reduced to 20.6 cc min$^{-1}$, the cold start effect is worse. For the other methanol supply rates of 15.8 and 11.0 cc min$^{-1}$, there appears to be an optimal parameter setting, although their effects are not comparable to the two optimal settings mentioned above. It is apparent from the above results that the temperature rise rate at the catalyst outlet of the methanol reformer is inversely proportional to the methanol supply rate under cold start condition, although the effect is less obvious for methanol supply rates of above 25.5 cc min$^{-1}$.

Fig. 5 shows the effect of heating temperature on the change in the outlet temperature of the catalyst from cold start for a methanol supply rate of 15.8–30.3 cc min$^{-1}$. Firstly, the effect of heating temperature on the time taken for the catalyst outlet temperature to reach 200 °C was investigated for the lowest

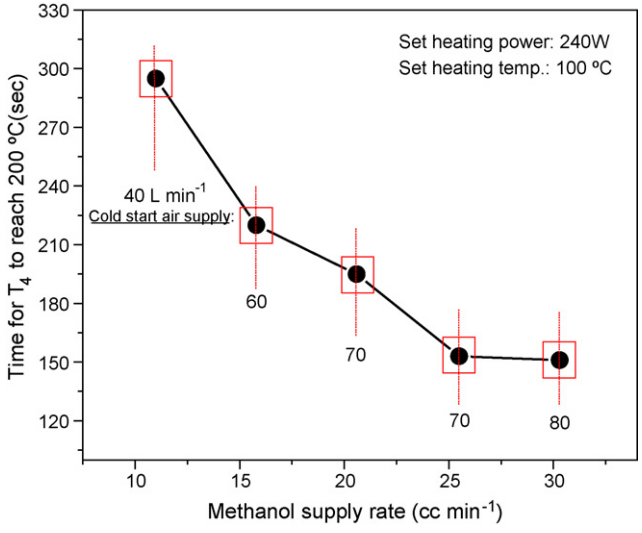


Fig. 4. Methanol supply rate on the time for $T_4$ to reach 200 °C under varying air supply rate from cold start for a heating power of 240 W.

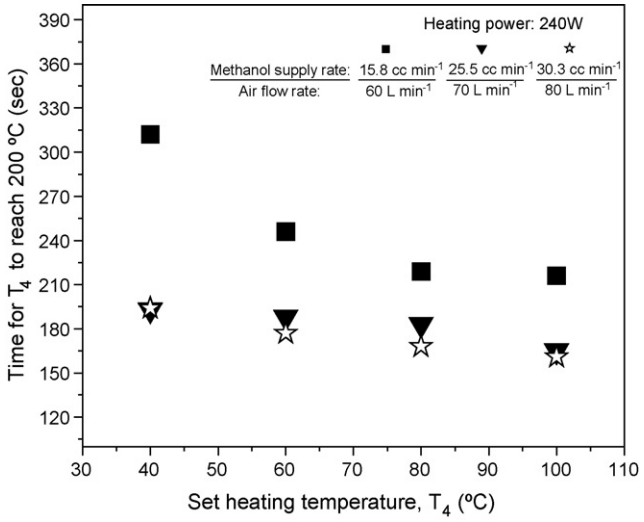


Fig. 5. Effect of pre-set heating temperature on the time for the outlet temperature of the catalyst to reach 200 °C for various methanol supply rate at 240 W heating power.

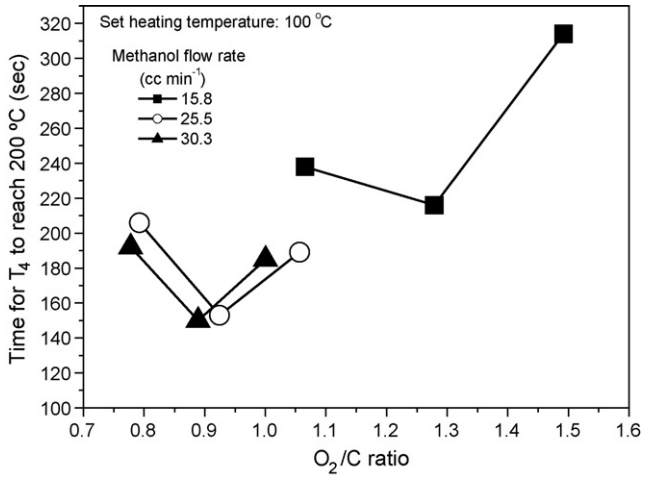


Fig. 6. Effect of $O_2$/C ratio on the time for $T_4$ to reach 200 °C from cold start under different methanol supply rate for a heating power of 240 W.

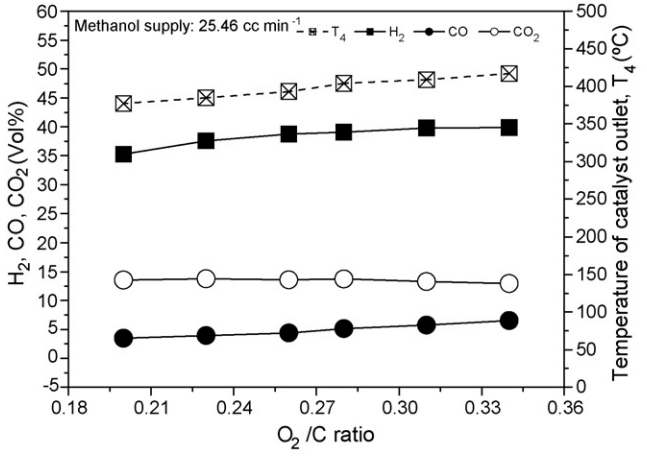


Fig. 7. Effect of $O_2$/C ratio on the steady produced gases and outlet temperature of catalyst for 25.5 cc min$^{-1}$ methanol supply rate.

methanol supply rate of 15.8 cc min$^{-1}$ in combination with an air flow supply rate of 60 L min$^{-1}$. It is evident that when the heating temperature is set at 100 °C, the optimal cold start effect is achieved and the time taken for the outlet temperature to reach 200 °C is about 216 s. This is similar for a heating temperature of 80 °C, which takes about 218 s but increases appreciably to about 246 s for 60 °C and to 314 s for 40 °C. Clearly, as the heating temperature setting is increased, the temperature rise rate at the catalyst outlet increases. The main reason being when the pre-set temperature is high, the corresponding oxidation period, and therefore heat dissipation period of the methanol is long, thereby resulting in the rapid rise of the catalyst temperature. The combined setting of a methanol supply rate of 25.5 cc min$^{-1}$, a heating power of 240 W, an air flow rate of 70 L min$^{-1}$, results in a generally similar trend as shown in Fig. 5, although the temperature rise at the catalyst outlet is much higher. This is particularly pronounced for the heating temperature of 100 °C where the time taken for the outlet temperature to reach 200°C is about 153 s, compared to the 80 °C pre-heat setting of about 185 s, the 60 °C setting of about 187 s and the 40 °C setting of about 191 s. Now, for the highest tested methanol supply rate of 30.3 cc min$^{-1}$ and a given air supply rate of 80 L min$^{-1}$, it is clear from Fig. 4 that the general trend is similar to the other two cases but with an even shorter time for the catalyst outlet temperature to reach 200 °C. The time taken in ascending order is: 150, 161, 171 and 192 s for the pre-set heating temperature of 100 °C, 80 °C, 60 °C and 40 °C. It is evident from this series of tests that the heating temperature of 100 °C results in the fastest response for all methanol supply rates, closely followed by the heating temperature of 80 °C.

Fig. 6 shows the effect of $O_2$/C ratio on the cold start response of the reformer system under different methanol supply rate for a heating power of 240 W. From this figure, it is observed that the $O_2$/C ratio during cold start is between 0.78 and 1.50, and that there exists an optimum value for each tested methanol supply rate. The best $O_2$/C ratio is around 1.28 for a methanol supply rate of 15.8 cc min$^{-1}$, and the time for $T_4$ to reach 200 °C from cold start is about 216 s. It is observed that these two optimum values decrease as methanol supply rate increases. However, as the methanol supply rate increasing from 25.5 cc min$^{-1}$ to 30.3 cc min$^{-1}$, these two values remain constant as shown in Fig. 4.

By using the optimum settings derived from the above analysis, i.e. a heating power of 240 W, a methanol supply rate of 25.5 cc min$^{-1}$ etc., the effect of the $O_2$/C ratio on the steady hydrogen production characteristics can be studied. From Fig. 7, it is evident that the catalyst outlet temperature increases with increasing $O_2$/C ratio, as does the hydrogen concentration. Above the $O_2$/C ratio of 0.26, however, the increase is less

Table 2
Enthalpy of reaction under different $O_2$/C ratios on the steady condition for 25.5 cc min$^{-1}$ methanol supply rate

| $O_2$/C | 0.23 | 0.26 | 0.28 | 0.31 | 0.34 |
|---|---|---|---|---|---|
| Enthalpy of reaction (kJ mol$^{-1}$) | −109.65 | −106.97 | −107.95 | −99.58 | −104.16 |

noticeable. Comparing the results in Table 2, it is clear that the differences of enthalpy of reaction between the $O_2$/C ratios of 0.26–0.34 were not obvious. This, however, allows a lower operating temperature to be selected and therefore, for subsequent tests, the $O_2$/C ratio of 0.26 was used.

Fig. 8 compares the effect of steady mode shifting temperature on the catalyst outlet temperature and the associated hydrogen production with time from cold start. The aim of testing at this temperature is to determine the quickest response from cold start with the least fuel consumption. Fig. 8(a) shows the effect of steady mode shifting temperature of between 30 °C and 250 °C at a pre-set heating temperature of 100 °C from cold start. At 30 °C, the rise in catalyst outlet temperature is gradual, reaching 57 °C after 240 s and achieving the maximum of 294 °C after 540 s. The rise in outlet temperature becomes more distinct when the steady mode shifting temperature is increased to 50 °C, with the increase clearly observed after 180 s and resulting in a final temperature of 343 °C. When the shifting temperature is increased beyond 75 °C, it is observed that the catalyst temperature could exceed 200 °C or even reaching 300 °C. However,

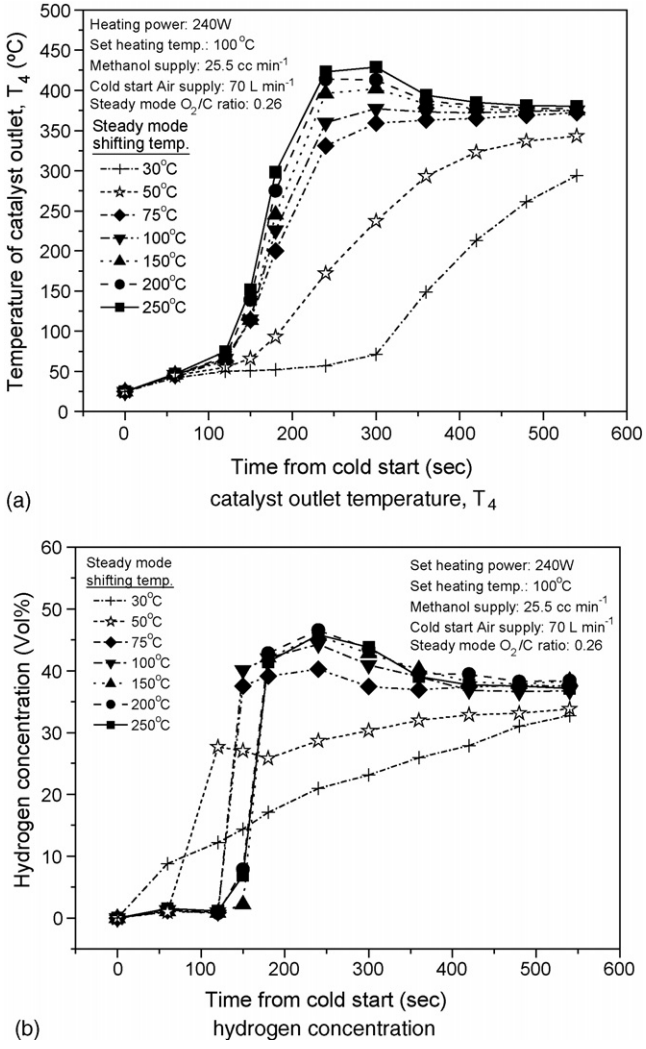


Fig. 8. Effect of steady mode shifting temperature on the outlet temperature of catalyst and hydrogen concentration during cold start.

Table 3
Equilibrium concentration of the produced gases under the steady mode shifting temperatures of 30 °C and 50 °C for 25.5 cc $min^{-1}$ methanol supply rate

| Steady mode shifting temperature (°C) | Concentration of the produced gases (%) | | | | | |
|---|---|---|---|---|---|---|
| | $H_2$ | CO | $CO_2$ | $N_2$ | $O_2$ | $CH_4$ |
| 30 | 32.8 | 3.0 | 15.7 | 43.3 | 0.34 | 4.86 |
| 50 | 33.8 | 3.4 | 15.2 | 42.2 | 0.31 | 5.04 |

it is clear that although the outlet temperature rise increases with the steady mode shifting temperature, the final steady temperature and the time to achieve that temperature are similar despite slight variations in the maximum temperatures. Now, upon inspecting the corresponding hydrogen-time histories in Fig. 8(b), it is observed that the steady mode shifting temperature of 30 °C and 50 °C results in rapid hydrogen production after 60 s and 120 s, respectively, due to an early lowering of the air flow rate. As the outlet temperature rise is gradual, as shown in Fig. 8(a), the rise in hydrogen is correspondingly slow with the final hydrogen concentration attaining only 33% at the steady mode shifting temperature of 30 °C and that for 50 °C a mere 34%. The equilibrium concentrations of the produced gases for these two temperatures are compared in Table 3. Amongst the other steady mode shifting temperatures, the time to hydrogen production is also longest for the 150–250 °C settings, whilst that for the settings of 75 and 100 °C is similar. Nevertheless, the time taken to achieve maximum hydrogen concentration and steady production for all cases of steady mode shifting temperature is similar. For the two pre-set heating temperatures, the hydrogen production history is comparable. Both reveal the quickest rise for the steady mode shifting temperature of 75 °C and 100 °C for the pre-set temperature range of 75–250 °C, and the final steady hydrogen concentration is similar at 38%, approximately.

From the results of Fig. 8(a) and (b), it is evident that the rise in catalyst outlet temperature increases with increasing steady mode shifting temperature at temperatures of under 75 °C. Notably, at a low steady mode shifting temperature, the production or generation of hydrogen is delayed and is also low in concentration. At very high steady mode shifting temperature, the reaction response is, however, not necessarily improved. It is clear that the steady mode shifting temperature of 75 °C and 100 °C results in the most rapid hydrogen production response with the final steady production concentration similar to that produced at higher steady mode shifting temperatures.

Figs. 9 and 10 show the analysis of the relationships of the steady mode shifting temperature and the time taken for the catalyst outlet temperature to reach 200 °C and the hydrogen concentration and flow rate at steady production, respectively, for a pre-set heating temperature of 65 °C and 100 °C. In Fig. 9, it is evident that with a steady mode shifting temperature of 30 °C and 50 °C, the time taken for the outlet temperature to reach 200 °C is significantly longer and the associated hydrogen production concentration and flow rate shown in Fig. 10 is low. At the higher temperatures of between 75 °C and 250 °C, the stable hydrogen production level is similar. It transpires therefore that there exists an optimum pre-set heating temperature to facilitate the response

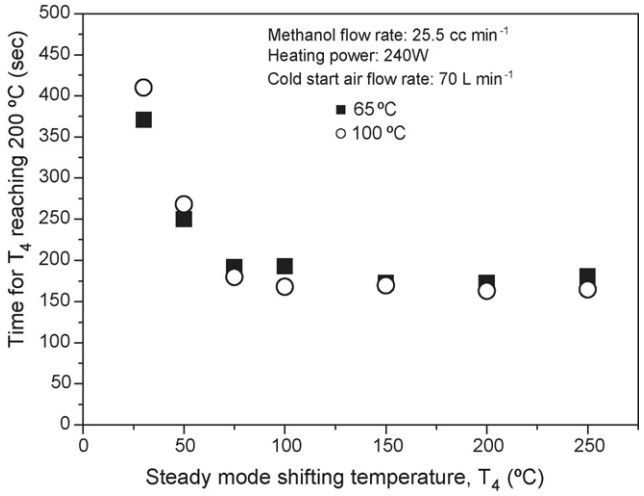


Fig. 9. Time for catalyst outlet temperature to reach 200 °C with steady mode shifting temperature for different set heating temperature.

of the catalyst as well as an optimum steady mode shifting temperature within the test range of the parameters and they are identified approximately as 65 °C and 75 °C, respectively.

### 3.2. Auto-thermal reforming

Figs. 11–13 show the response from the transient reaction of partial oxidation to auto-thermal reforming for an S/C ratio of 0.68, 0.90 and 1.29, respectively. The fixed settings are a methanol supply rate of 25.5 cc $min^{-1}$ and an $O_2$/C ratio of 0.20. It is evident from Fig. 11 that the reformer reaches stability from cold start at 430 s. Notably, the S/C ratio is zero at this instant as there is no water intake. When water is injected at about 475 s, the partial oxidation process is transformed into auto-thermal reforming. It is apparent from the figure the temperatures within the reformer at $T_1$ (pre-fuel injection), $T_2$ (post fuel injection), and $T_3$ (the catalyst inlet temperature) decrease due to the latent heat absorption by the intake water. On the other hand, $T_4$ (the catalyst outlet temperature) will rise slightly from heat dissipated from water gas shifting. In terms of emission, the hydrogen concentration rises as does $CO_2$ by 5% and

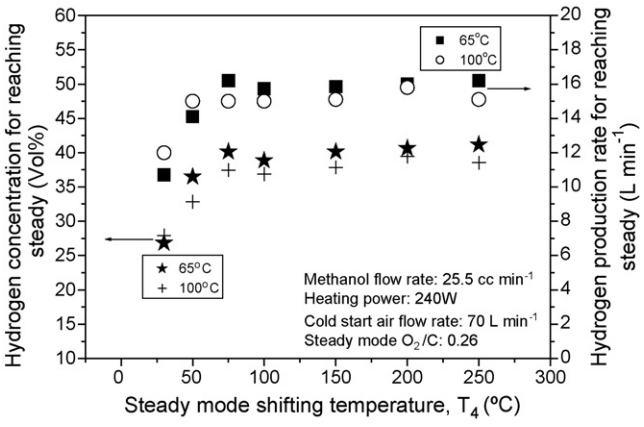


Fig. 10. Effect of steady mode shifting temperature on steady hydrogen concentration and flow rate production for different set heating temperatures.

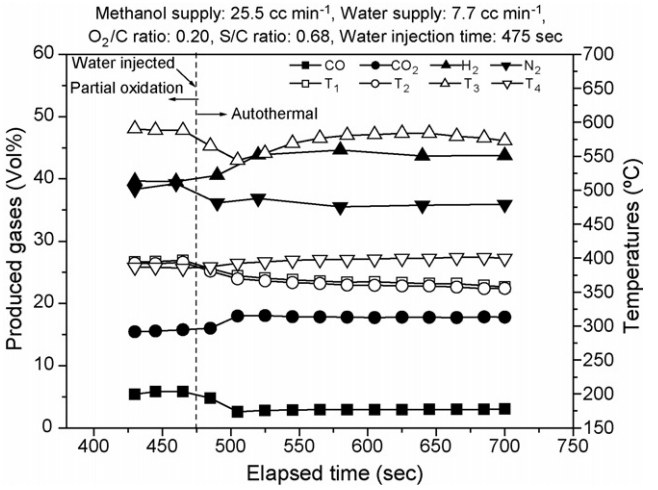


Fig. 11. Transient reaction from partial oxidation to auto-thermal reforming for an S/C ratio of 0.68.

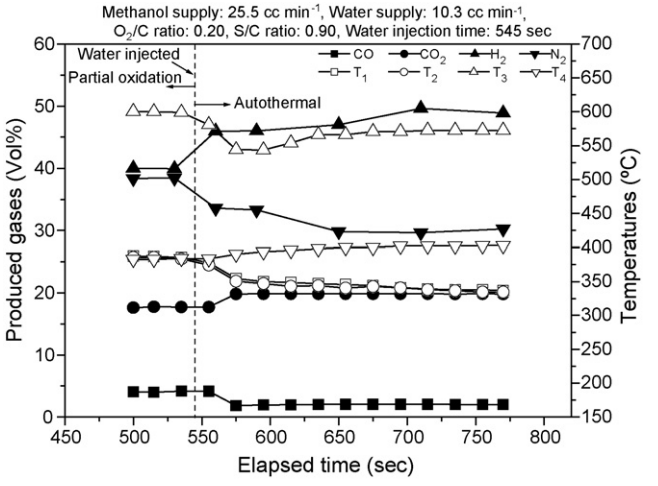


Fig. 12. Transient reaction from partial oxidation to auto-thermal reforming for an S/C ratio of 0.90.

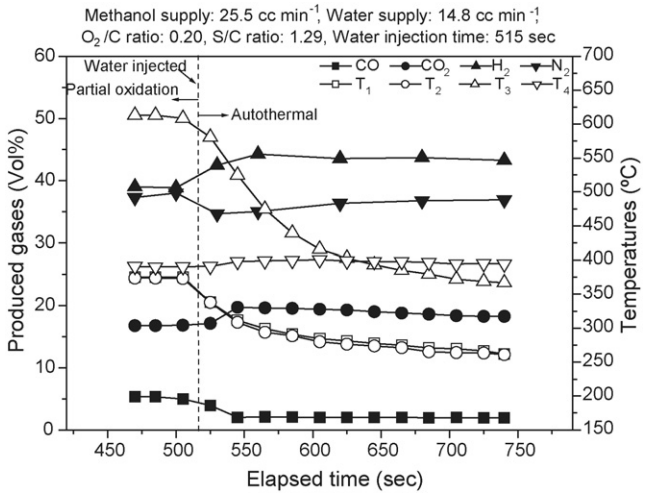


Fig. 13. Transient reaction from partial oxidation to auto-thermal reforming for an S/C ratio of 1.29.

2.11%, respectively. The CO and $N_2$ concentration decrease by about 3.04% and 4.11%, respectively. In the transformation from partial oxidation to auto-thermal reforming, increased $CO_2$ and hydrogen are formed from the reaction of CO in the reformed gas with water vapour during water gas shifting. In general, the temperature changes within the reformer and the rate of change of the emission composition during the transfer process commence around 5 s after water is injected and stabilize after about 40 s. When the S/C ratio is increased to 0.90, it is evident from Fig. 12 that at 545 s after water is injected into the reformer, the temperature within the reformer exhibits similar trend to Fig. 11. In other words, $T_1$, $T_2$ and $T_3$ decrease slightly while $T_4$ increases. The emission composition is similar with increase in hydrogen and $CO_2$ of 10.31% and 2.22%, respectively, while the CO and $N_2$ concentration decrease by 2.25% and 9.24%, respectively. The same trends are observed in Fig. 13, with the highest S/C ratio of 1.29. After partial oxidation is transformed into auto-thermal reforming, water vapour is injected into the reformer at 515 s. However, as the S/C ratio is of the highest value, the amount of water vapour injection is highest. This results in a more pronounced decrease in $T_1$, $T_2$ and $T_3$ while the increase in $T_4$ is marginal. The emission increase in hydrogen and $CO_2$ is 5.14% and 2.02%, respectively, and the corresponding decrease in CO and $N_2$ concentration is 3.21% and 2.28%. It is apparent that the temperature variations of the reformer and the change in emission composition in this setting are similar to Figs. 11 and 12 and that these transient changes, which occur at about 5 s after the transfer of the process, are rapid. The main finding from varying the S/C ratio is that the optimum transient response is obtained under an S/C ratio of 0.90, which produced the highest hydrogen concentration of 49.12%.

The general conclusion from the above series of tests is that after stabilization from cold start, the $H_2$ and $CO_2$ gas emissions of the reformer clearly improve in the transient period between the transformation from partial oxidation to auto-thermal reforming and the corresponding CO emission, on the other hand, reduces appreciably. This suggests that the process transfer is complete and that the transient response is swift.

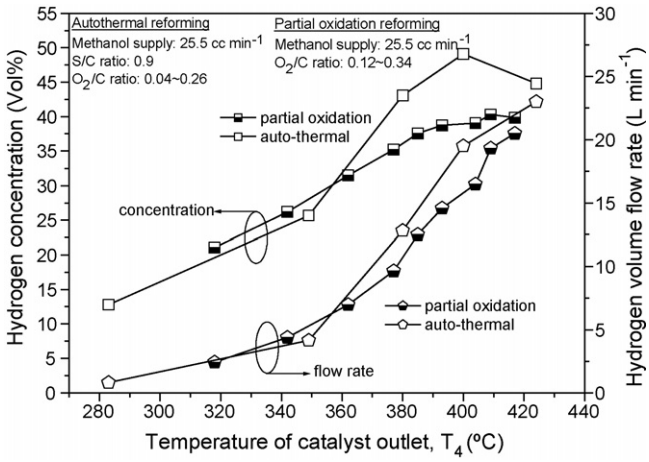


Fig. 14. Comparison of hydrogen production by partial oxidation and auto-thermal reforming.

Fig. 14 compares the characteristics of hydrogen produced by partial oxidation and by auto-thermal reforming. It is clear from the figure that at temperatures beyond 360 °C, the hydrogen concentration and mass flow rate produced by auto-thermal reforming are both higher than by partial oxidation. Under this temperature, these two quantities are lower for auto-thermal reforming although for both processes these quantities are all less than 25% and 5 L $min^{-1}$, respectively. At the start of auto-thermal reforming when water is injected, a lower temperature is observed as some of the heat generated is absorbed by the water as latent heat. At a temperature of 283 °C, the hydrogen concentration is only about 12.8% but increases as the temperature rises. At about 400 °C, the hydrogen concentration reaches its peak. The same trend is observed for the hydrogen

Table 4
Comparison of different fuel processors during cold start

| Author(s) [Ref] | Fuels | Size (kW) | Specific power (kW $kg^{-1}$) | Cold start strategy | Start-up time (s) | Power input during cold start (kW) | $O_2$/C (inlet) | S/C (inlet) |
|---|---|---|---|---|---|---|---|---|
| Han [2] | Methanol | 3.0 | 0.6 | – | >300 | – | – | – |
| Springmann [16] | Gasoline | – | – | Electric heating<br>POX<br>ATR | 150 | 33 | 0.24 | 2.0 |
| Goebel [17] | Gasoline | 68 | 1.94 | Oxidation ($H_2$ or fuel)<br>ATR | 140[a]<br>190[b] | 18.6 | 0.415 | 1.8 |
| Ahmed [18] | Gasoline | 10 | 0.7 | POX<br>ATR | <600[c]<br><60[d] | 48.3 | 0.325 | 2.1 |
| This study | Methanol | 4.36 | 0.5[e] | Electric heating<br>POX<br>ATR | 220 | 6.62[f] | 0.20–0.26 | 0.68–1.29 |

[a] Fuelled with hydrogen for catalyst light-off.
[b] Fuelled with C$x$H$y$ for catalyst light-off ($x$ = 7.494, $y$ = 14.53).
[c] Status of 2003.
[d] Target of 2005.
[e] Could be improved by reducing the number of flanges.
[f] Including 0.24 kW of heating power (before light-off).

production rate, i.e. it increases rapidly with temperature. Under auto-thermal reforming, the maximum hydrogen concentration produced is 49.12% with a corresponding hydrogen mass flow rate of 23.0 L $min^{-1}$(4.36 kW). This is much higher than the 40.0% and 20.5 L $min^{-1}$ (3.89 kW) produced by partial oxidation. The best thermal efficiency for the partial oxidation reforming when operated at stable condition is about 60.36%, and that for the auto-thermal reforming is about 60.0%. In this process, however, the hydrogen mass flow rate increased too rapidly with temperature that testing was stopped at a high temperature to avoid damaging the catalyst.

Further, the comparison of different fuel processors during cold start is shown in Table 4. In this Table, it can be found that their objectives focused on accelerating the start-up of the fuel processors. The common strategy was getting the catalyst to light-off rapidly by (partial) oxidation, and then switching to auto-thermal reforming. It was also found that the response of the reformer improved year by year. In this study, there is the potential to improve the cold start by reducing the mass of the reformer and changing the ceramic to a metallic substrate. However, the effects of thermal shock and cycling on durability must be considered.

## 4. Conclusions

From a series of tests of the pre-set heating temperature, methanol supply rate, steady mode shifting temperature on the temperature rise and the hydrogen production characteristics of a methanol reformer by partial oxidation and auto-thermal reforming, a few conclusions can been drawn.

The tests revealed an optimum pre-set heating temperature and an optimum steady mode shifting temperature for facilitating the most rapid response of the catalyst of the reformer. Further, it was shown that the catalyst outlet temperature rise increased more rapidly for a higher steady mode shifting temperature. That is, there existed an optimum temperature range for shifting to steady operation from a transient cold start. When the steady mode shifting temperature was set too low, the hydrogen production response was slow with the final production level lower than when the steady mode shifting temperature was high. When the steady mode shifting temperature was too high, however, the response was not rapid. Within the optimum temperature range for the steady mode shifting, the quickest hydrogen production response was obtained and the final steady hydrogen production level was similar to that produced under higher steady mode shifting temperature. It was concluded thus that the optimum steady mode shifting temperature of this test set-up was approximately 75 °C. Further, the hydrogen concentration produced by auto-thermal could be as high as 49.12% and the volume flow rate up to 23.0 L $min^{-1}$ compared to 40.0% and 20.5 L $min^{-1}$ produced by partial oxidation. The improvement in the volume flow rate is approximately 15%.

## Acknowledgements

The authors are grateful to the support of the National Science Council of Taiwan under grant number NSC 91-2212-E-168-015 and NSC 93-2212-E-168-013. Special thanks are also due to the Heterogeneous Catalysis Department in the Material and Chemical Laboratories of the Industrial Technology Research Institute for providing the catalyst for testing.

## References

[1] Y.T. Cheng, C.K. Yang, H.T. Su, J. Energy 25 (1995) 158–180.
[2] J.S. Han, I.S. Kim, K.S. Choi, J. Power Sources 86 (2000) 223–227.
[3] L.Y. Sung, J. Energy 24 (1994) 69–88.
[4] L.Y. Sung, J. Energy 24 (1994) 96–116.
[5] H.C. Chen, Study on the Hydrogen Generation by the Methanol Reformer for a PEM Fuel Cell, Master Thesis of Department of Aeronautics and Astronautics of National Cheng Kung University, Taiwan, 2002.
[6] B. Höhlein, M. Boe, J. Bøgild-Hansen, P. Bröckerhoff, G. Colsman, B. Emonts, J. Power Sources 61 (1996) 143–147.
[7] B. Emonts, J. Bøgild-Hansen, S.L. Jørgensen, B. Höhlein, R. Peters, J. Power Sources 71 (1998) 288–293.
[8] W. Wiese, B. Emonts, R. Peters, J. Power Sources 84 (1999) 187–193.
[9] S. Nagano, H. Miyagawa, O. Azegami, K. Ohsawa, Energy Convers. Manage. 42 (2001) 1817–1829.
[10] K. Takeda, A. Baba, Y. Hishinuma, T. Chikahisa, JSAE Rev. 23 (2002) 183–188.
[11] Y. Choi, H.G. Stenger, Appl. Catal. B: Environ. 38 (2002) 259–269.
[12] J.D. Holladay, E.O. Jones, M. Phelps, J. Hu, J. Power Sources 108 (2002) 21–27.
[13] B. Lindström, L.J. Pettersson, J. Power Sources 118 (2003) 71–78.
[14] D.G. Löffler, K. Taylor, D. Mason, J. Power Sources 117 (2003) 84–91.
[15] R.F. Horng, Energy Convers. Manage. 46 (2005) 1193–1207.
[16] S. Springmann, M. Bohnet, A. Docter, A. Lamm, G. Eigenberger, J. Power Sources 128 (2004) 13–24.
[17] S.G. Goebel, D.P. Miller, W.H. Pettit, M.D. Cartwright, Int. J. Hydrogen Energy 30 (2005) 953–962.
[18] S. Ahmed, R. Ahluwalia, S.H.D. Lee, S. Lottes, J. Power Sources 154 (2006) 214–222.
[19] R.F. Horng, C.R. Chen, T.S. Wu, C.H. Chan, Appl. Therm. Eng. 26 (2006) 1115–1124.